Perifornical Urocortin-3 mediates the link between stress-induced anxiety and energy homeostasis

Yael Kuperman, Orna Issler, Limor Regev, Ifat Musseri, Inbal Navon, Adi Neufeld-Cohen, Shosh Gil, and Alon Chen[1]

Department of Neurobiology, Weizmann Institute of Science, Rehovot 76100, Israel

Communicated by Wylie W. Vale, The Salk Institute for Biological Studies, La Jolla, CA, March 24, 2010 (received for review November 3, 2009)

In response to physiological or psychological challenges, the brain activates behavioral and neuroendocrine systems linked to both metabolic and emotional outputs designed to adapt to the demand. However, dysregulation of integration of these physiological responses to challenge can have severe psychological and physiological consequences, and inappropriate regulation, disproportional intensity, or chronic or irreversible activation of the stress response is linked to the etiology and pathophysiology of mood and metabolic disorders. Using a transgenic mouse model and lentiviral approach, we demonstrate the involvement of the hypothalamic neuropeptide Urocortin-3, a specific ligand for the type-2 corticotropin-releasing factor receptor, in modulating septal and hypothalamic nuclei responsible for anxiety-like behaviors and metabolic functions, respectively. These results position Urocortin-3 as a neuromodulator linking stress-induced anxiety and energy homeostasis and pave the way toward better understanding of the mechanisms that mediate the reciprocal relationships between stress, mood and metabolic disorders.

metabolic disorders | mood disorders | corticotropin-releasing factor (CRF) | CRF receptor type 2 | stress response

In modern Western societies, the high stress load correlates with an increasing incidence of mood disorders and metabolic syndrome, both of which have reached epidemic proportions over the past decades (1, 2). Exposure to acute or chronic stress is associated with derangement of metabolic and behavioral homeostasis that contributes to the clinical presentation of visceral obesity, type 2 diabetes, atherosclerosis, and metabolic syndrome (2–4). The corticotropin-releasing factor (CRF) neuropeptide system is the primary central mediator of the stress response and contributes to the etiology of stress-related psychiatric illness (5–8). Studies conducted using CRF receptor type 2 (CRFR2)-null mice or Urocortin-2 (Ucn2)-null mice provided evidence that, in addition to its role in mediating stress-related behavior, central CRFR2 is important in modulating metabolic rate, appetite, and feeding behaviors (9–12).

The Urocortin-3 (Ucn3) neuropeptide selectively binds and activates CRFR2. Ucn3 is expressed predominately within the hypothalamus, in the median preoptic nucleus and the rostral perifornical area (rPFA) (13–15). The major rPFA-Ucn3 terminal fields, the lateral septum (LS) and the ventromedial hypothalamus (VMH), express high levels of CRFR2 (15). Different stressors and homeostatic insults influence Ucn3 expression levels, suggesting its position as a potential modulator of the stress response (13, 16).

To assess the functional relevance of endogenous rPFA–Ucn3 neuronal pathways, activating the CRFR2 both in the LS and the VMH, in mediating behavioral and metabolic responses to challenge, we used a site-specific and inducible genetic approach in vivo. We report that rPFA-Ucn3 overexpression induces an anxiety-like behavior, increases the respiratory exchange ratio (RER) and heat production, and influences all-body glucose metabolism.

Results and Discussion

Establishment of Site-Specific and Inducible Ucn3-Overexpressing Mouse Model. To evaluate the importance of rPFA-Ucn3 expression in mediating stress-induced behavioral and metabolic changes, we used a site-specific and inducible genetic approach in vivo. We used the Tet-On gene expression system which enables us to regulate gene expression in a precise, reversible, and quantitative manner (17, 18). To that end, we generated a mouse model that overexpresses Ucn3 under the control of tetracycline responsive element (TRE) promoter (Ucn3-TRE) (Fig. 1*A*). To obtain an inducible overexpression of Ucn3, we generated lentiviruses that constitutively express the reverse-tetracycline transactivator (rtTA) and GFP, which serves as a reporter (Fig. 1*A*). We chose to manipulation the rPFA because it highly expresses Ucn3 (13, 14) and its major Ucn3 terminal fields, the LS and the VMH (15), express high levels of CRFR2 (19) and are implicated in anxiety-like behaviors and metabolic functions, respectively (20–22). Site-specific delivery of the rtTA lentiviruses into the rPFA of Ucn3-TRE mice (Fig. 1*B*) generates an inducible system that, after administration of drinking water containing doxycycline (Dox) (Fig. 1*C*), allows site-specific Ucn3 overexpression and stronger Ucn3 innervations to its CRFR2-containing terminal fields (Fig. 1 *B* and *C*).

To confirm the ability of the rtTA-expressing lentiviral vectors to activate the TRE promoter, before its in vivo application, we used the luciferase reporter system and generated TRE-luciferase–expressing vector (Fig. 2*A*). Only HEK293T cells transfected with both TRE-luciferase and rtTA-expressing constructs demonstrated robust and inducible activation of the luciferase gene following exposure to Dox (Fig. 2*B*). The Ucn3 endogenous expression site was verified using radioactive in situ hybridization (Fig. 2*C*, *Middle*), and immunostaining with anti GFP antibody was used to verify the lentiviral injection site (Fig. 2*C*, *Right*). Ucn3-TRE mice injected with rtTA lentiviruses specifically into the rPFA showed an apparent increase in Ucn3 immunoreactive-containing fibers (Fig. 1 *E* and *F*), which overlap with the CRFR2 mRNA expression demonstrated using CRFR2-specific in situ hybridization (Fig. 1*D*). In addition, Ucn3 mRNA levels determined using real-time PCR demonstrated a 3-fold increase following Dox administration (Fig. 2*D*).

Receptors expression levels often are down-regulated in response to continuous ligand administration (23). In the current study, rPFA-Ucn3 overexpression did not alter CRFR2 expression levels in either rPFA terminal fields, the septum (Fig. S1*A*) and hypothalamus (Fig. S1*B*), or in other unconnected neuroanatomical sites such as the medial amygdala (Fig. S1*B*). Additionally, activation of the PFA–LS–VMH pathways did not modify the endogenous levels of Ucn3 expressed in the medial amygdala (Fig. S1*D*) and the bed nucleus of the stria terminalis (Fig. S1*E*).

A Robust Increase in Anxiety-Like Behavior in Mice Overexpressing Ucn3 Specifically at the rPFA. In light of the suggested connection

Author contributions: Y.K. and A.C. designed research; Y.K., O.I., L.R., I.M., I.N., A.N.-C., S.G., and A.C. performed research; Y.K., O.I., and A.C. analyzed data; and Y.K. and A.C. wrote the paper.

The authors declare no conflict of interest.

[1]To whom correspondence should be addressed. E-mail: alon.chen@weizmann.ac.il.

This article contains supporting information online at www.pnas.org/cgi/content/full/1003969107/DCSupplemental.

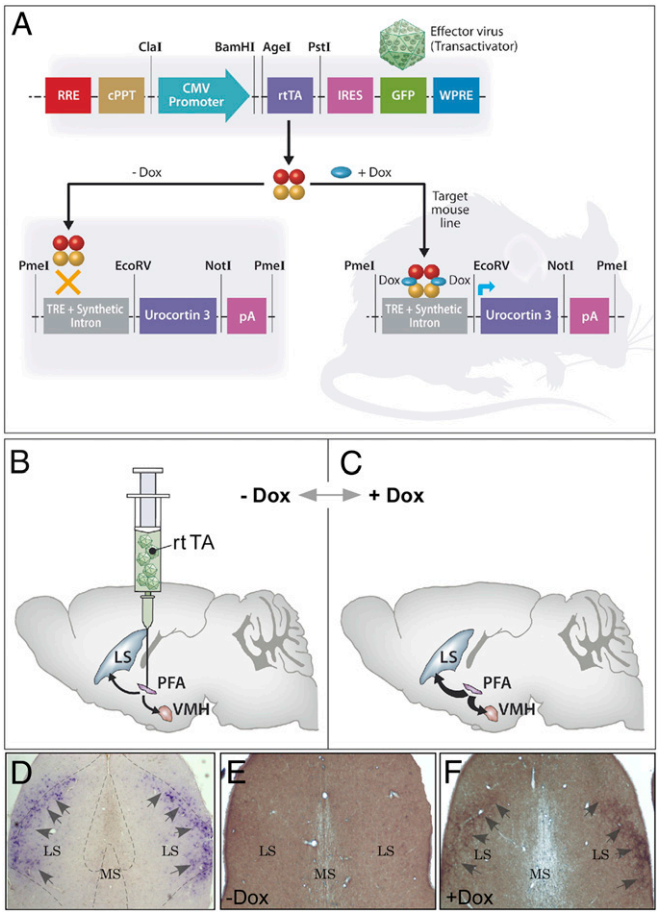

Fig. 1. Establishment of site-specific and inducible Ucn3-overexpressing transgenic mouse model. (*A*) Schematic representation of the tetracycline-responsive regulatory system for transcriptional transactivation in a combined transgenic mouse and lentiviral systems. (*B* and *C*) Injection of the transactivator ('effector virus') into a specific site of the transgenic mouse brain will result in incorporation of the reverse transactivator (rtTA)-expressing sequence at the infected neuron, ensuring constant and stable expression. In the presence of the inducer doxycycline (Dox), the rtTA protein binds TRE and activates transcription of Ucn3 at the injection site. The rtTA lentiviruses were injected to the rPFA, which endogenously expresses Ucn3 and projects to the LS and the VMH. In the presence of Dox, rPFA-Ucn3 is overexpressed, and its release at the LS and VMH nuclei is intensified. (*D*–*F*) Immunostaining of lateral septal Ucn3 terminal fields. In situ hybridization demonstrating lateral septal CRFR2 mRNA expression, indicated by arrowheads (*D*). Immunostaining for lateral septal Ucn3 terminal fields (fibers immunostaining, indicated by arrowheads) obtained from mouse that was not treated (*E*) or was treated (*F*) with Dox. RRE, Rev-responsive element; cPPT, central polypurine tract; WPRE, Woodchuck hepatitis post-transcriptional regulatory element; CMV, cytomegalovirus; IRES, internal ribosome entry site; pA, polyadenylation site.

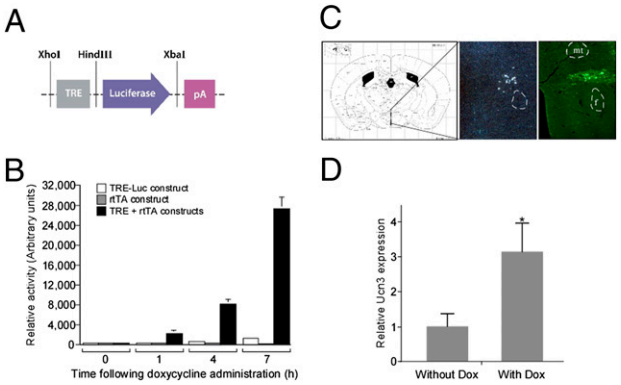

Fig. 2. Verification of rtTA-expressing lentiviruses, rPFA-Ucn3 injection site, and Ucn3 mRNA levels. (*A*) Schematic representation of the luciferase reporter construct designed and used for in vitro verification studies in HEK293T cells. Luciferase expression is controlled by TRE and activated in the presence of both rtTA and Dox. (*B*) HEK293T cells transfected with both TRE-luciferase and rtTA-expressing constructs demonstrated an inducible activation of the luciferase gene following exposure to Dox. (*C*) Brain coronal section adapted from the Paxinos & Franklin mouse brain atlas (49), showing the PFA location (*Left*), a specific Ucn3 radioactive in situ hybridization indicating Ucn3-expressing cells in the rPFA (*Middle*), and the site of lentiviral injection as verified by immunostaining using anti-GFP antibody (*Right*). (*D*) Ucn3 mRNA levels in mouse brain with or without exposure to Dox. f, fornix; pA, polyadenylation site. *, $P < 0.05$.

between behavioral and metabolic alterations in response to challenge, mice overexpressing Ucn3 specifically at the rPFA were tested for both anxiety-like behavior and metabolic adjustments. It is important to note that anxiety disorders and depression often co-occur, and the onset of depression frequently is observed following a long period of anxiety (24). To evaluate the anxiety-like behavior of mice overexpressing Ucn3 at the rPFA, we performed a set of anxiety-related behavioral tests under induced (+Dox) or noninduced (−Dox) conditions. Mice overexpressing rPFA-Ucn3 display a robust increase in anxiety-like behavior, as measured by both the open-field and the dark–light transfer tests. In the open-field test (Fig. 3 *A*–*D*), mice overexpressing Ucn3 spent less time in the center of the arena ($t_{(9)} = -3.152$; $P < 0.01$) (Fig. 3*A*), showed longer latencies to enter the center ($t_{(9)} = -2.316$; $P < 0.05$) (Fig. 3*B*), visited the center less ($t_{(9)} = -2.733$; $P < 0.05$) (Fig. 3*C*), and traveled less distance during the test ($t_{(9)} = -2.322$; $P < 0.05$) (Fig. 3*D*). In the dark–light transfer test (Fig. 3 *E*–*G*, mice overexpressing Ucn3 showed longer latencies to enter the light compartment ($t_{(9)} = 3.334$; $P < 0.01$) (Fig. 3*E*), tended to spend less time in the light compartment ($t_{(9)} = -2.215$; $P = 0.054$) (Fig. 3*F*), and made fewer transitions between the compartments ($t_{(9)} = -2.93$; $P < 0.05$) (Fig. 3*G*). No changes were observed in general home-cage locomotion (Fig. 3*H*), suggesting that the observed anxiogenic phenotype in these mice is not caused by altered locomotor activity.

The VMH nuclei are known to be involved in food intake, energy expenditure, and female sexual behavior (25) but are not thought to mediate anxiety-like behavior. Therefore, we can assume that the behavioral effects were mediated by overactivation of CRFR2 in the LS. Our results are in agreement with previous pharmacological studies indicating that LS-CRFR2 activation mediates increased anxiety-like behavior (26, 27).

Although inducible expression of transgenes using the Tet-On system is a well-established genetic tool (17, 18), and previous studies have demonstrated the inert effect of Dox on body temperature (28) and on learning- and memory-related tasks (29, 30), we further confirmed that Dox administration to wild-type mice did not affect the behavioral and metabolic parameters tested in the current study (Figs. S2 and S3).

Increased Metabolic Rate in Mice Overexpressing rPFA-Ucn3. We assessed the metabolic effects of mice overexpressing Ucn3 at the rPFA before and after exposure to the inducer Dox. Overexpression of rPFA-Ucn3 did not affect food intake during the light or dark phase of the day cycle (Fig. 4*A*). Indirect calorimetry was used to determine whether rPFA-Ucn3 overexpression alters their energy expenditure or substrate utilization. We found that overexpression of rPFA-Ucn3 mediated a significant increase in the RER (Fig. 4*B*). Using a repeated-measurements two-way ANOVA, a main effect for Dox treatment was found ($F_{Dox(1,14)} = 6.887$; $P < 0.05$), and post hoc Student's *t* test showed significant elevation during both the light and the dark (active) phase of the

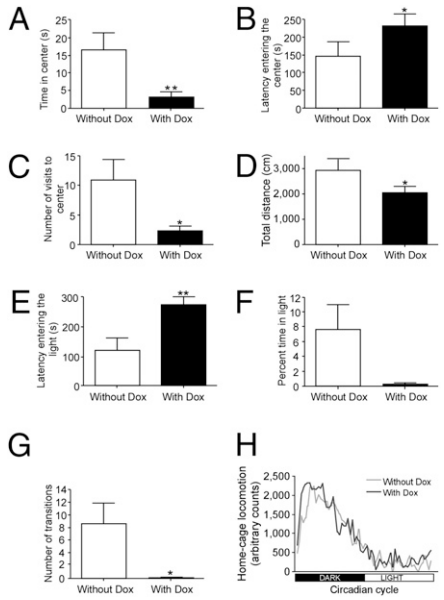

Fig. 3. Ucn3 overexpression at the rPFA increases anxiety-like behavior. (*A–D*) Anxiety-like behavior of rPFA-Ucn3 overexpressing animals as measured by the open-field test. Time spent in the center of the arena (*A*), latency entering the center (*B*), visits to the center (*C*), and distance traveled during the test (*D*) are indicative of increase in anxiety-like behavior. (*E–G*) Anxiety-like behavior as measured by the dark–light transfer test. The latency entering the light compartment (E), percentage of time spent in the light compartment (*F*), and number of transitions into the light compartment (*G*) are indicative of anxiogenic behavior. (*H*) Home-cage locomotor activity was similar in the two experimental conditions. *, $P < 0.05$; **, $P < 0.01$ vs. without Dox (paired Student's *t* test). Values are expressed as the mean ± SEM ($n = 10$ mice per group).

day cycle. (RER: light cycle −Dox: 0.732 ± 0.019; +Dox: 0.775 ± 0.012; $t_{(26)} = -2.07$; $P < 0.05$; dark cycle: −Dox: 0.809 ± 0.012; +Dox 0.854 ± 0.014; $t_{(26)} = -2.18$; $P < 0.05$) (Fig. 4*C*). The increased RER indicates that mice overexpressing rPFA-Ucn3 oxidize more carbohydrate as a fraction of the total energy consumed. Because mice ate chow diet throughout the experiment, the increased RER does not reflect changes in food choice but rather an inner change in carbohydrate vs. fatty acid oxidation ratio. In addition, there was a significant augmentation in oxygen consumption (VO_2) (Fig. 4*D*), carbon dioxide production (VCO_2) (Fig. 4*E*), and dark-cycle heat production (Fig. 4*F*), indices of whole-body energy expenditure. Heat production was elevated during both the dark and the light cycles; repeated-measurements two-way ANOVA showed a main effect for Dox treatment ($F_{Dox(1,14)} = 6.201$; $P < 0.05$), and post hoc Student's *t* test showed significant elevation during the dark cycle [heat production (kcal/h/kg): light cycle −Dox: 10.46 ± 0.54; +Dox: 11.84 ± 0.30; $t_{(19)} = -2.07$; $P = 0.052$; dark cycle: −Dox: 13.99 ± 0.50; +Dox: 15.87 ± 0.50; $t_{(19)} = -2.83$; $P < 0.05$] (Fig. 4*F*). Overall, we found that rPFA-Ucn3 overexpression modulates metabolism but not food intake. Overexpression of rPFA-Ucn3 induces an increase in the metabolic rate throughout the day, but no changes were observed in locomotor activity (Fig. 4 *G* and *H*).

CRFR2 ligands have been proposed as anorectic agents (31–33). Although Ucn1 injection to the LS and Ucn3 injection to the VMH produced an anorectic effect (26, 34), overexpression of rPFA-Ucn3, in this study, had no such effect. This difference may be explained by dose differences; the effects mentioned were produced using pharmacological Ucn3 doses. It has been shown in rats that an increase in anxiety-like behaviors mediated by Ucn1 infusion to the LS is produced by doses lower than those required to reduce food intake (250 ng vs. 500 ng per animal) (26). In our paradigm, the secreted dose may be high enough to induce the behavioral and metabolic changes we observed but too low to exert an anorectic effect. In addition, when we expose the mice to Dox, we observe a continuous effect of Ucn3 expression which might differ from the acute one. Because the observed increase in heat production is not a consequence of increased activity, it may relate to a pathway shared by leptin and CRFR2 in the VMH. Intra-VMH injection of Ucn3 causes an anorectic phenotype, that is similar to i.c.v. leptin administration (34) and is known to increase energy expenditure (35). The increased heat production also may reflect an increase in sympathetic flow, which may be mediated via the activation of the VMH (36, 37). It was demonstrated previously that electrical stimulation of the VMH activates brown adipose tissue thermogenesis (38) and increases blood pressure and heart rate (39). Activation of the sympathetic system also could be mediated via the PFA projections to the paraventricular nucleus (40), a key source of autonomic outflow. Ucn1 administration to the paraventricular nucleus influences the expression of uncoupling proteins in the brown adipose tissue (41). Interestingly, following psychosocial stress, dominant mice also exhibited increased dark-cycle heat production without changes in locomotor activity or food intake (42).

Decreased Insulin Sensitivity in Mice Overexpressing Rpfa-Ucn3. Glucose- and insulin-tolerance tests were performed to determine whether rPFA-Ucn3 overexpression also modulates changes in whole-body glucose homeostasis. Overexpression of rPFA-Ucn3 did not influence glucose tolerance in mice (Fig. 4*I*). However, insulin-tolerance test measurements demonstrated a significant reduction in insulin sensitivity compared with rPFA-rtTA–injected mice that did not receive Dox in their drinking water (Fig. 4*J*). Interestingly, this observation is in agreement with the reported Ucn3-null mouse phenotype, which demonstrated improved glucose and insulin tolerance while kept on a high-fat diet (43).

After 30 days of Dox administration, mice overexpressing PFA-Ucn3 tended to have a higher body weight ($P = 0.071$) (Fig. S4*A*). However, body composition analysis revealed that mice do not differ by the percentage of fat or lean mass (Fig. S4*B*). Postmortem analysis found similar liver weight with no overt or histological signs of fatty liver (Fig. S4 *C* and *D*). Interestingly, although β-islet morphology, determined by insulin staining, was comparable in the two experimental groups (Fig. S4*E*), insulin levels were significantly elevated in mice overexpressing rPFA-Ucn3 (Fig. 4*K*).

Previous studies have demonstrated the involvement of VMH-CRFR2 in central regulation of glucose homeostasis (44, 45). Acute administration of Ucn3 directly into the VMH increased both plasma glucose and insulin levels (45), further supporting the hyperinsulinemia observed in the present study. Additionally, given the reduced insulin sensitivity, the hyperinsulinemia may represent a compensatory mechanism by which the pancreas compensates by secreting increased levels of insulin, and, as a result, glucose clearance (examined by the glucose-tolerance test) remains unchanged. In patients with type 2 diabetes, insulin resistance and hyperinsulinemia precede the onset of the disease (46, 47). In our paradigm, exposure to PFA-Ucn3 for 20 days was sufficient to drive the organism to a prediabetic state. These data emphasize the relationship between continuous stress and its metabolic consequences.

In summary, our results clearly demonstrate the involvement of rPFA-Ucn3–expressing neurons in regulating anxiety-like behaviors, energy expenditure, and whole-body glucose metabolism. The current study strongly suggests a role for rPFA-Ucn3 in mediating the link between stress-induced anxiety and energy homeostasis and positions the Ucn3 and the CRFR2 central pathways as major components of the brain response to psychological and/or physiological challenge. Here we observed a single

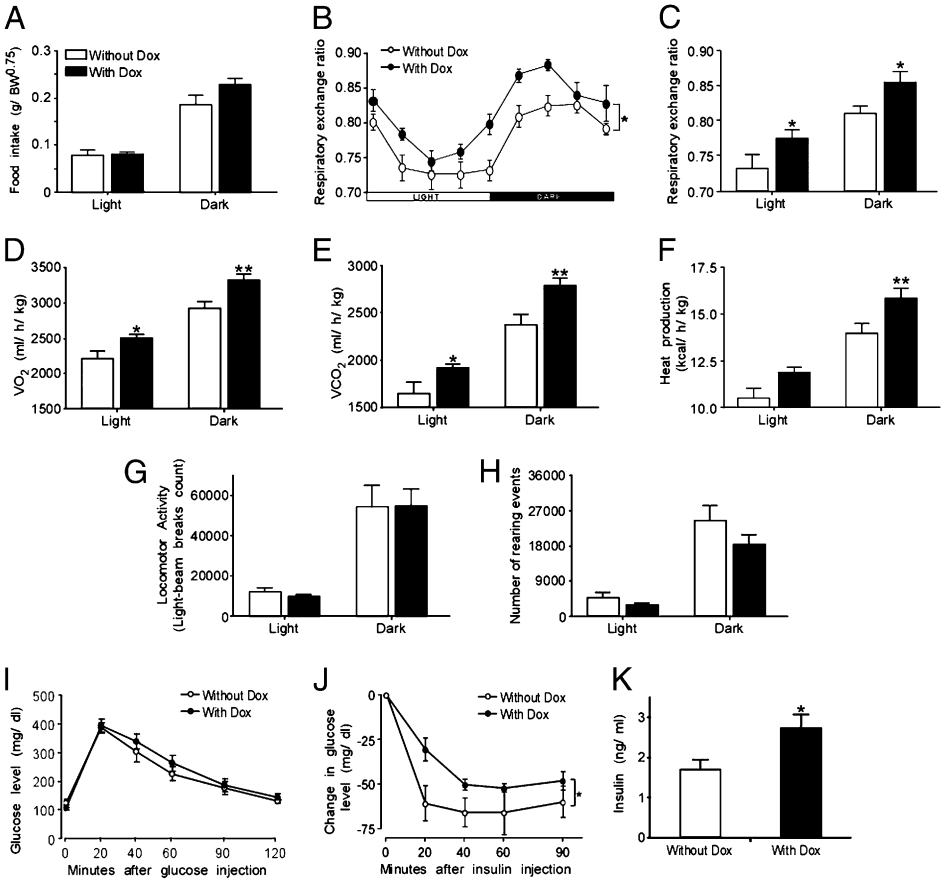

Fig. 4. Metabolic alterations in the conditional rPFA-Ucn3–overexpressing transgenic mice. (*A*) Food intake, (*B*) RER profile; (*C*) RER averaged values, (*D*) oxygen consumption (VO_2), (*E*) carbon dioxide production (VCO_2), (*F*) heat production, (*G*) locomotor activity, and (*H*) rearing events were measured continuously and simultaneously. Significant differences in RER, VO_2, VCO_2, and in heat production following rPFA-Ucn3 overexpression were observed (n = 8–10 mice per group). (*I and J*) All-body glucose homeostasis determined using glucose-tolerance test (*I*) and insulin-tolerance test (*J*) in mice treated with or without Dox demonstrates normal glucose tolerance but reduce insulin sensitivity. Mice (n = 6–11 per group) were injected i.p. with 2 g glucose/kg body weight (BW) (*I*) or with 0.75 U insulin/kg BW (J), and plasma glucose was measured at the indicated time points. (*K*) Insulin plasma level. Values are expressed as the mean ± SEM *, $P < 0.05$ **, $P < 0.01$ vs. without Dox (repeated measurements two-way ANOVA).

neuropeptide, expressed by a defined neuronal population, that is responsible for mediating both behavioral and metabolic responses, which collectively promote coping responses to challenge. These data may pave the way toward better understanding of the mechanisms that mediate the reciprocal relationships between stress, mood disorders, and energy homeostasis.

Methods

Animal Care. Mice were maintained in a pathogen-free temperature-controlled (22 ± 1 °C) mouse facility on a reverse 12-h light-dark cycle at The Weizmann Institute of Science, according to institutional guidelines. Food and water were given ad libitum. All experimental protocols were approved by the Institutional Animal Care and Use Committee of The Weizmann Institute of Science.

Establishment of Conditional and Site-Specific Ucn3-Overexpressing Transgenic Mouse Model. DNA vector containing the target (TRE-Ucn3) nucleotide sequence was constructed as follows: Mouse (m) Ucn3 cDNA (GeneBank accession no. AF361944) was PCR amplified from pmUcnIII(0.6)-pCRII-TOPO vector (kindly provided by Wylie Vale, Salk Institute for Biological Studies, La Jolla, CA). The following oligonucleotide primers were used for the PCR isolation of mUcn3: sense primer: 5′-GTTTCACATCCTTCTTTTCTAC-3′ and the antisense primer: 5′-CTTGTCTTGATGTGCCACCCTC-3′, carrying restriction sites for *EcoRV* and *NotI*, respectively. The purified PCR product, containing the full coding sequence of mUcn3, was cloned downstream to a TRE-containing plasmid (kindly provided by Charles Zuker, University of California, San Diego, La Jolla, CA), using the *EcoRV* and *NotI* restriction sites. A linearized DNA fragment of ≈1.7 kb (using 5′ and 3′ *PmeI* restriction sites) containing the TRE, Ucn3 cDNA, and a PolyA signal was injected into fertilized oocytes and produced four lines of BALBC/C57/B6 background mice (AC1014, AC1021, AC1025, and AC1029). All four lines demonstrated stable germline transmission of the transgene. Lines AC1021 and AC1029 exhibited higher levels of Ucn3, compared with the wild-type endogenous levels, under noninduced conditions and were excluded from this study. To determine the ability of the AC1014 and AC1025 lines to overexpress Ucn3 conditionally, mice were centrally injected with rtTA-expressing lentiviruses and, following a 1-week recovery period, were treated with Dox or were not treated. Both lines exhibited a significant increase in Ucn3 expression following Dox administration observed by both RT-PCR and immunostaining.

Luciferase Construct and Assays. TRE was PCR-cloned into pGL3-basic vector (Promega Corp.) using *XhoI* and *HindIII* restriction sites. HEK293T cells were transiently transfected using polyethylenimine with TRE-luciferase vector, rtTA-expressing vector, or both vectors. β-gal–expressing plasmid was cotransfected as an internal control for transfection efficiency. Cells were harvested 1, 4, or 7 h after Dox treatment, and cell lysates were analyzed for luciferase activity in a luminometer (Veritas; Turner BioSystems). Luminescence was measured for 5 s immediately after addition of luciferin assay buffer. Transfections were performed at least three times (in 4–6 replicates) for each construct or treatment tested. Luciferase activities were normalized to β-gal activity.

Lentiviral Vector Construction, Production, and Experimental Groups. Recombinant pseudotyped lentiviral vectors were generated by cotransfection of four plasmids into HEK293T cells and were concentrated by ultracentrifugation, as described previously (48). Mice were anesthetized with ketamine (100 mg/kg)/acepromazine (4 mg/kg)/xylazine (10 mg/kg) administered i.p. Mice were

injected bilaterally using a 1-μL Hamilton syringe with 1 μL lentiviruses expressing the rtTA protein into each side of the rostral perifornical area (injection coordinates: bregma, −0.94 mm; medial-lateral, ±0.67 mm; and dorso-ventral, 1.05 mm). Lentiviral injections were conducted using a computer-guided stereotaxic instrument and a motorized nanoinjector (Angle Two Stereotaxic Instrument; myNeurolab), which is fully integrated with the Paxinos mouse brain atlas (49) via a control panel. Mice were given a 2-week period for recovery. For the behavioral and metabolic cage studies, 15 mice were injected and tested before and after the exposure to Dox. For the glucose- and insulin-tolerance tests a second group of 23 mice was injected, 12 of which were kept on Dox. Data of five mice from the first group and six mice from the second group were excluded because of inaccurate injections. A third group of 16 mice was injected to examine the CRFR2 and Ucn3 expression levels at specific brain nuclei.

RNA Preparation and Real-Time PCR. rtTA-injected mice treated with or without Dox-containing drinking water for 20 days were decapitated. The brains were removed and placed immediately into a 1-mm metal matrix (Stoelting Co.). The brain was sliced using standard razor blades (GEM; Personna American Safety Razor Co.), into 2-mm slices that were quickly frozen on dry ice. The area of interest was punched using a microdissecting needle of an appropriate size and stored at −80°C. RNA was extracted using a 5 PRIME PerfectPure RNA Cell & Tissue kit (5 Prime GmbH). RNA preparations were reverse transcribed to generate cDNA using High Capacity cDNA Reverse Transcription Kit (Applied Biosystems Inc.). The cDNA products were used as templates for Real-Time PCR analysis. Sense and antisense primers were selected to be located on different exons to avoid false-positive results caused by DNA contamination. The following specific primers were designed using Primer Express software (Applied Biosystems, Perkin-Elmer). For mCRFR2: 5′-TACCGAATCGCCCTCATTGT-3′ and 5′-CCACGCGATGTTTCTCAGAAT-3′ corresponding to nucleotides 479–498 and 640–620, respectively (GenBank accession no. AY445512); for mUcn3: 5′-CTCCTGGCCCGGAAGC-3′ and 5′-CATCAGCATCGCTCCCTGT-3′ corresponding to nucleotides 444–459 and 524–506, respectively (GenBank accession no. NM_031250.5). For mouse hypoxanthine guanine phosphoribosyl transferase 1 (HPRT1), which served as an internal control: 5′-GCAGTACAGCCCCAAAATGG-3′ and, 5′-GGTCCTTTTCACCAGCAAGCT-3′ corresponding to nucleotides 599–618 and 650–630, respectively (GenBank accession no. NM_013556). Real-time PCR reactions were carried out on a 7500 Real-Time PCR system using fluorescent SYBR Green technology (Applied Biosystems Inc.). Reaction protocols had the following format: 10 min at 95 °C for enzyme activation followed by 45 cycles of 15 s at 94 °C and 60 s at 60 °C. The specificity of the amplification products was checked by melting curve analysis. All reactions contained the same amount of cDNA, 10 μL Master Mix and 250 nM primers to a final volume of 20 μL.

Histological and Immunohistological Analysis. Animals were anesthetized and perfused with phosphate-buffered 4% paraformaldehyde. Fixed brains were serially sectioned , and confirmation of the accuracy of the injection site was done by immunostaining using biotinylated anti GFP antibody raised in rabbit as primary antibody (Abcam.) and streptavidin conjugated Cy2 anti rabbit as secondary antibody (Jackson ImmunoResearch Laboratories, Inc.). Immunostaining for Ucn3 was done using anti-rabbit Ucn3 antibody (kindly provided by Wylie Vale, Salk Institute for Biological Studies, La Jolla, CA), using the standard ABC staining method according to the manufacturer's instructions (Vector Laboratories). The presence of Ucn3 was visualized using DAB peroxidase (Sigma-Aldrich). For insulin staining, pancreata were dissected and fixed in 1% paraformaldehyde for 24 h at 4 °C. Fixed pancreata then were embedded into paraffin blocks. Sections 3–5 μm thick were deparaffinized and rehydrated. Anti-insulin antibody raised in guinea pig (DAKO U.K. Ltd.) was used as primary antibody, and Cy3-conjugated anti-guinea pig antibody served as a secondary antibody (Jackson ImmunoResearch Laboratories, Inc.). Mayer's H&E staining was done by standard procedure.

In Situ Hybridization. Ucn3 in situ hybridization was performed as previously described (50). For CRFR2 in situ hybridization, antisense and sense (control) RNA probes were generated using CRFR2α cDNA and labeled with DIG-11-UTP using a labeling kit (Roche Molecular Biochemicals). In situ hybridization for CRFR2α mRNAs was carried out with the free-floating section method as previously described (51).

Doxycycline Administration. Lentiviral-injected mice were tested for a variety of physiological and behavioral parameters, both under basal condition (−Dox) or following exposure to Dox in their drinking water (0.5 mg/mL + 0.2% sucrose) (+Dox). Notably, this dose is relatively low compared with other studies (28–30). Parallel studies showed no sequence or practice effects in the behavioral tests. For testing the effect of Dox on wild-type mice, 16 male CB6 mice were assigned randomly to two groups, one of which was exposed to Dox as described above. Mice were tested for their behavioral and metabolic performances.

Behavioral Studies. All behavioral studies were performed during the dark phase following habituation to the test room for 2 h before any test. For the assessment of anxiety-like behaviors, the open field and the light–dark transfer were used. The open field consisted of a Plexiglas box (50 × 50 × 22 cm). The arena was illuminated with 120 lux. Each mouse was placed in the corner of the apparatus to initiate a 10-min test session. The time spent in the center of the arena, the latency to cross the center, the number of entries into the arena center, and the total distance traveled were measured. The light–dark transfer test consists of two compartments, a dark compartment (14 × 27 × 26 cm) and a compartment illuminated by 1050 lux (30 × 27 × 26 cm), connected by a small passage. Mice were placed in the dark compartment to initiate a 5-min test session. The time spent in the light compartment, the number of entries to the light compartment, and the latency of entering the light zone were measured. The indices collected in these tests were quantified using an automated video tracking system (VideoMot2; TSE Systems).

Metabolic Studies. Indirect calorimetry, food and water intake, and locomotor activity were measured using the Labmaster system (TSE Systems). The LabMaster instrument consists of a combination of sensitive feeding and drinking sensors for automated online measurement. The calorimetry system is an open-circuit system that determines O_2 consumption, CO_2 production, and RER. A photobeam-based activity monitoring system detects and records ambulatory movements, including rearing and climbing, in every cage. All the parameters are measured continuously and simultaneously. Data were collected after 48 h of adaptation in acclimated singly housed mice.

Glucose- and Insulin-Tolerance Tests. Glucose- and insulin-tolerance tests were performed as previously described (11, 52). Briefly, following 4 h of fasting, glucose (2g/kg of body weight) was injected i.p., and whole venous blood obtained from the tail vein at 0, 20, 40, 60, 90, and 120 min after the injection was measured for glucose by using an automatic glucometer (One Touch; Lifescan). For the insulin-tolerance test, fasting mice were injected with insulin (0.75 units/kg of body weight; Sigma), and blood glucose levels were measured before and at 20, 40, 60, and 90 min after insulin injection.

Body Composition. Body composition was assessed using Echo-MRI (Echo Medical Systems).

Insulin Quantification. Insulin levels were determined using an ultrasensitive insulin ELISA immunoassay kit (Chrystal Chem).

Statistical Analysis. Results are expressed as means ± SEM. Statistical analysis was performed using repeated-measurements two-way ANOVA with post hoc Student's *t* tests or paired Student's *t* tests, as appropriate using JMP software (SAS).

ACKNOWLEDGMENTS. We thank Cindy Donaldson (The Salk Institute, La Jolla, CA) for technical assistance. A.C. is incumbent of the Philip Harris and Gerald Ronson Career Development Chair. This work is supported by the Minerva Foundation with funding from the Federal German Ministry for Education and Research, a D-Cure Fellowship, research grants from the Israel Science Foundation, the National Institute for Psychobiology in Israel (founded by the Charles E. Smith Family), the Israel Ministry of Health, Roberto and Renata Ruhman, Jorge David Ashkenazi, Mr. and Mrs. Barry Wolfe, the Nella and Leon Benoziyo Center for Neurosciences, and a grant from Mr. and Mrs. Mike Kahn.

1. Charmandari E, Tsigos C, Chrousos G (2005) Endocrinology of the stress response. *Annu Rev Physiol* 67:259–284.
2. Kyrou I, Tsigos C (2007) Stress mechanisms and metabolic complications. *Horm Metab Res* 39:430–438.
3. Dallman MF, et al. (2003) Chronic stress and obesity: A new view of "comfort food". *Proc Natl Acad Sci USA* 100:11696–11701.
4. Carroll D, et al. (2009) Generalized anxiety disorder is associated with metabolic syndrome in the Vietnam experience study. *Biol Psychiatry* 66:91–93.
5. Bale TL, Vale WW (2004) CRF and CRF receptors: Role in stress responsivity and other behaviors. *Annu Rev Pharmacol Toxicol* 44:525–557.
6. Dautzenberg FM, Hauger RL (2002) The CRF peptide family and their receptors: Yet more partners discovered. *Trends Pharmacol Sci* 23:71–77.

7. de Kloet ER, Joëls M, Holsboer F (2005) Stress and the brain: From adaptation to disease. *Nat Rev Neurosci* 6:463–475.
8. Reul JM, Holsboer F (2002) Corticotropin-releasing factor receptors 1 and 2 in anxiety and depression. *Curr Opin Pharmacol* 2:23–33.
9. Bale TL, et al. (2003) Corticotropin-releasing factor receptor-2-deficient mice display abnormal homeostatic responses to challenges of increased dietary fat and cold. *Endocrinology* 144:2580–2587.
10. Bale TL, et al. (2000) Mice deficient for corticotropin-releasing hormone receptor-2 display anxiety-like behaviour and are hypersensitive to stress. *Nat Genet* 24:410–414.
11. Chen A, et al. (2006) Urocortin 2 modulates glucose utilization and insulin sensitivity in skeletal muscle. *Proc Natl Acad Sci USA* 103:16580–16585.
12. Coste SC, et al. (2000) Abnormal adaptations to stress and impaired cardiovascular function in mice lacking corticotropin-releasing hormone receptor-2. *Nat Genet* 24: 403–409.
13. Jamieson PM, Li C, Kukura C, Vaughan J, Vale W (2006) Urocortin 3 modulates the neuroendocrine stress response and is regulated in rat amygdala and hypothalamus by stress and glucocorticoids. *Endocrinology* 147:4578–4588.
14. Lewis K, et al. (2001) Identification of urocortin III, an additional member of the corticotropin-releasing factor (CRF) family with high affinity for the CRF2 receptor. *Proc Natl Acad Sci USA* 98:7570–7575.
15. Li C, Vaughan J, Sawchenko PE, Vale WW (2002) Urocortin III-immunoreactive projections in rat brain: Partial overlap with sites of type 2 corticotrophin-releasing factor receptor expression. *J Neurosci* 22:991–1001.
16. Venihaki M, et al. (2004) Urocortin III, a brain neuropeptide of the corticotropin-releasing hormone family: Modulation by stress and attenuation of some anxiety-like behaviours. *J Neuroendocrinol* 16:411–422.
17. Gossen M, Bujard H (1992) Tight control of gene expression in mammalian cells by tetracycline-responsive promoters. *Proc Natl Acad Sci USA* 89:5547–5551.
18. Gossen M, et al. (1995) Transcriptional activation by tetracyclines in mammalian cells. *Science* 268:1766–1769.
19. Van Pett K, et al. (2000) Distribution of mRNAs encoding CRF receptors in brain and pituitary of rat and mouse. *J Comp Neurol* 428:191–212.
20. Eckart K, et al. (1999) Actions of CRF and its analogs. *Curr Med Chem* 6:1035–1053.
21. Eghbal-Ahmadi M, Avishai-Eliner S, Hatalski CG, Baram TZ (1999) Differential regulation of the expression of corticotropin-releasing factor receptor type 2 (CRF2) in hypothalamus and amygdala of the immature rat by sensory input and food intake. *J Neurosci* 19: 3982–3991.
22. Nishiyama M, Makino S, Asaba K, Hashimoto K (1999) Leptin effects on the expression of type-2 CRH receptor mRNA in the ventromedial hypothalamus in the rat. *J Neuroendocrinol* 11:307–314.
23. Sakakibara H, Taga M, Ikeda M, Kurogi K, Minaguchi H (1996) Continuous stimulation of gonadotropin-releasing hormone (GnRH) receptors by GnRH agonist decreases pituitary GnRH receptor messenger ribonucleic acid concentration in immature female rats. *Endocr J* 43:115–118.
24. Müller MB, Wurst W (2004) Getting closer to affective disorders: The role of CRH receptor systems. *Trends Mol Med* 10:409–415.
25. McClellan KM, Parker KL, Tobet S (2006) Development of the ventromedial nucleus of the hypothalamus. *Front Neuroendocrinol* 27:193–209.
26. Bakshi VP, Newman SM, Smith-Roe S, Jochman KA, Kalin NH (2007) Stimulation of lateral septum CRF2 receptors promotes anorexia and stress-like behaviors: Functional homology to CRF1 receptors in basolateral amygdala. *J Neurosci* 27: 10568–10577.
27. Todorovic C, et al. (2007) Differential activation of CRF receptor subtypes removes stress-induced memory deficit and anxiety. *Eur J Neurosci* 25:3385–3397.
28. Stark KL, Gross C, Richardson-Jones J, Zhuang X, Hen R. (2007) A novel conditional knockout strategy applied to serotonin receptors. *Handb Exp Pharmacol* (178):347–363.
29. Mansuy IM, et al. (1998) Inducible and reversible gene expression with the rtTA system for the study of memory. *Neuron* 21:257–265.
30. Shimizu E, Tang YP, Rampon C, Tsien JZ (2000) NMDA receptor-dependent synaptic reinforcement as a crucial process for memory consolidation. *Science* 290:1170–1174.
31. Bradbury MJ, McBurnie MI, Denton DA, Lee KF, Vale WW (2000) Modulation of urocortin-induced hypophagia and weight loss by corticotropin-releasing factor receptor 1 deficiency in mice. *Endocrinology* 141:2715–2724.
32. Zorrilla EP, et al. (2004) Human urocortin 2, a corticotropin-releasing factor (CRF)2 agonist, and ovine CRF, a CRF1 agonist, differentially alter feeding and motor activity. *J Pharmacol Exp Ther* 310:1027–1034.
33. Inoue K, et al. (2003) Human urocortin II, a selective agonist for the type 2 corticotropin-releasing factor receptor, decreases feeding and drinking in the rat. *J Pharmacol Exp Ther* 305:385–393.
34. Fekete EM, et al. (2007) Delayed satiety-like actions and altered feeding microstructure by a selective type 2 corticotropin-releasing factor agonist in rats: Intrahypothalamic urocortin 3 administration reduces food intake by prolonging the post-meal interval. *Neuropsychopharmacology* 32:1052–1068.
35. Pelleymounter MA, et al. (1995) Effects of the obese gene product on body weight regulation in ob/ob mice. *Science* 269:540–543.
36. Swanson LW, Kuypers HG (1980) A direct projection from the ventromedial nucleus and retrochiasmatic area of the hypothalamus to the medulla and spinal cord of the rat. *Neurosci Lett* 17:307–312.
37. Haque MS, et al. (1999) Role of the sympathetic nervous system and insulin in enhancing glucose uptake in peripheral tissues after intrahypothalamic injection of leptin in rats. *Diabetes* 48:1706–1712.
38. Perkins MN, Rothwell NJ, Stock MJ, Stone TW (1981) Activation of brown adipose tissue thermogenesis by the ventromedial hypothalamus. *Nature* 289:401–402.
39. Thornhill J, Halvorson I (1993) Intrascapular brown adipose tissue (IBAT) temperature and blood flow responses following ventromedial hypothalamic stimulation to sham and IBAT-denervated rats. *Brain Res* 615:289–294.
40. Ziegler DR, Herman JP (2002) Neurocircuitry of stress integration: Anatomical pathways regulating the hypothalamo-pituitary-adrenocortical axis of the rat. *Integr Comp Biol* 42:541–551.
41. Kotz CM, Wang C, Levine AS, Billington CJ (2002) Urocortin in the hypothalamic PVN increases leptin and affects uncoupling proteins-1 and -3 in rats. *Am J Physiol Regul Integr Comp Physiol* 282:R546–R551.
42. Moles A, et al. (2006) Psychosocial stress affects energy balance in mice: Modulation by social status. *Psychoneuroendocrinology* 31:623–633.
43. Li C, Chen P, Vaughan J, Lee KF, Vale W (2007) Urocortin 3 regulates glucose-stimulated insulin secretion and energy homeostasis. *Proc Natl Acad Sci USA* 104: 4206–4211.
44. McCrimmon RJ, et al. (2006) Corticotrophin-releasing factor receptors within the ventromedial hypothalamus regulate hypoglycemia-induced hormonal counterregulation. *J Clin Invest* 116:1723–1730.
45. Chen P, Vaughan J, Donaldson C, Vale W, Li C. (2010) Injection of Urocortin 3 into the ventromedial hypothalamus modulates feeding, blood glucose levels and hypothalamic POMC gene expression but not the HPA axis. *Am J Physiol Endocrinol Metab*, 10.1152/ajpendo.00402.2009.
46. Warram JH, Martin BC, Krolewski AS, Soeldner JS, Kahn CR (1990) Slow glucose removal rate and hyperinsulinemia precede the development of type II diabetes in the offspring of diabetic parents. *Ann Intern Med* 113:909–915.
47. Petersen KF, Shulman GI (2002) Pathogenesis of skeletal muscle insulin resistance in type 2 diabetes mellitus. *Am J Cardiol* 90(5A):11G–18G.
48. Tiscornia G, Singer O, Verma IM (2006) Production and purification of lentiviral vectors. *Nat Protoc* 1:241–245.
49. Paxinos G, Franklin KBJ (2001) *The Mouse Brain in Stereotaxic Coordinates* (Academic, San Diego).
50. Chen A, et al. (2006) Urocortin 2-deficient mice exhibit gender-specific alterations in circadian hypothalamus-pituitary-adrenal axis and depressive-like behavior. *J Neurosci* 26:5500–5510.
51. Neufeld-Cohen A, et al. (2010) Urocortin-1 and -2 double-deficient mice show robust anxiolytic phenotype and modified serotonergic activity in anxiety circuits. *Mol Psychiatry* 15:426–441.
52. Kuperman Y, Chen A (2008) Urocortins: Emerging metabolic and energy homeostasis perspectives. *Trends Endocrinol Metab* 19:122–129.